Detection of permanent open water surfaces in central Siberia with ENVISAT ASAR wide swath data with special emphasis on the estimation of methane fluxes from tundra wetlands

Short title: Open water surfaces in central Siberia

Annett Bartsch[1], Carsten Pathe[1], Klaus Scipal[1,2], Wolfgang Wagner[1]

1) Institute of Photogrammetry and Remote Sensing, Vienna University of Technology
Gusshausstraße 27-29, 1040 Vienna, Austria
Tel: +43-(0)1-58801-12221, Fax: +43-(0)1-58801-12299, E-mail: ab@ipf.tuwien.ac.at

2) now at ECMWF, Reading, UK

Abstract

Permanent water bodies not only store dissolved CO_2 but are essential for the maintenance of wetlands in their proximity. Under the view point of greenhouse gas (GHG) accounting wetland functions comprise sequestration of carbon under anaerobic conditions and methane release. The investigated area in central Siberia covers boreal and sub-arctic environments. Small inundated basins are abundant on the sub-arctic Taymir lowlands but also in parts of severe boreal climate where permafrost ice content is high and feature important freshwater ecosystems. Satellite radar imagery (ENVISAT ScanSAR) acquired in summer 2003 and 2004, have been used to derive open water surfaces with 150 m resolution, covering an area of approximately 3 Mio km². The open water surface maps were derived using a simple threshold based classification method. The results were assessed with Russian forest inventory data, which includes detailed information about water bodies. The resulting classification has been further used to estimate the extent of tundra wetlands and to determine their importance for methane emissions. Tundra wetlands cover 7% (400,000 km²) of the study region and methane emissions from hydromorphic soils are estimated to be 45,000 t day^{-1} for the Taymir peninsula.

Keywords: remote sensing, ScanSAR, Siberia, Taymir, tundra, wetland

Introduction

Freshwater ecosystems constitute wetlands, which play an important role as sink or source of greenhouse gases (GHGs). Wetlands are dynamic and are affected by climate change, as are albedo and fresh water fluxes in the arctic system (Callaghan *et al.* 2004). Their exact role as sink or source is still uncertain especially over Siberia (Friborg *et al.* 2003).

There have been several attempts to map freshwater ecosystems globally. One recent effort was the creation of the Global Lakes and Wetlands Database (Lehner and Döll 2004). It is based on a collection of data bases ranging from digital maps to text records on local, regional and global scale. Therefore the accuracy varies considerably between different locations and minimum feature size is 10 ha. Another useful source for deriving information about water bodies are satellite data, which provide global coverage and a fair spatial resolution. Additionally satellite data can provide up to date information on permanent inundation. Products with 300 m resolution were created using multi spectral data within initiatives such as GLOBCOVER (http://dup.esrin.esa.int/news/news58.asp, July 2004). This information is recent, but fairly coarse with a minimum detectable feature size of 15 ha. McCallum *et al.* (2006) have compared various globally available land cover maps derived from satellite data, identifying an extremely low agreement of the different products over Russia. Frey and Smith (2007) exemplify the poor performance of those data sets for wetlands and water bodies within the West Siberian Lowlands. More accurate data is therefore needed especially for vast and remote regions such as Siberia.

Wetlands act as important sinks and sources of CO_2, CH_4 and other GHGs in northern latitudes. Current ecosystem models concentrate on CO_2. Methane, which is the second most important GHG, is still scarcely considered. Approximately 20% of global methane emissions originate from natural wetlands (Mitra *et al.* 2005). Emissions are temperature sensitive and have increased between 22-66% between 1970 and 2000 over some sub-arctic wetlands in Scandinavia (Christensen *et al.* 2003). Russian methane emissions account for more than half of the global emissions (Stolbovoi *et al.* 2004). Emissions occur especially in fens but also from shallow lakes of the Siberian tundra biome. The sediments which act as source originate from the Pleistocene and emission from them accounts for half of annual methanogenesis in this region (Zimov *et al.* 1997). Apart from the incomplete account of greenhouse gases, global climate models consider open water surfaces and wetlands in their function for humidification of the atmosphere and thus indirectly impact the carbon cycle only on continental scale (Krinner 2003).

The present work has been carried out within the framework of the Siberia II project, which deals with multi-sensor concepts for greenhouse gas accounting in northern Eurasia (Schmullius *et al.* 2003). The study area comprises about 3 Mio km² and stretches south-north from Lake Baikal to Taymir peninsula (Fig. 1). Satellite radar images acquired by the European ENVIronmental SATellite (ENVISAT) are used to derive permanently inundated basins. The density of those lakes is used for the delineation of Tundra wetland area.

The aim of this study is to

1) test a radar image based approach for inundation mapping over large areas,
2) update and improve the existing land cover database in central Siberia,
3) derive wetland information important for GHG accounting, especially for estimating methane emissions in the subarctic environment,
4) estimate methane fluxes for tundra wetlands within the SIBERIA II project area, and
5) provide a base for monitoring fresh water ecosystems.

Study area and freshwater ecosystems

The SIBERIA II study area is located in central Siberia and covers tundra, boreal and steppe environment (Fig. 1). It includes the transition zone from continuous to non-permafrost and maritime to continental climate. The southern Taimyr Peninsula features a very important and extensive tundra fresh water ecosystem. Three Ramsar wetlands of international importance can be found in this moderate sub-arctic environment. The largest is Pura/Gorbitta covering 26,000 km². Most of the bigger lakes on Taymir peninsula have been formed by thermokarst processes related to high ground ice content (Tumel 2002), e.g. lake Labaz (Andreev *et al.* 2002) and lake Middendorf (Laing and Smol 2003). Permafrost depth ranges from 300 to 600 m. During summer, water tables are less than 10 cm below the ground surface in the valleys (Schmidt and Bölter 2002). The active layer depth increased in this region during the last 20 years, when anthropogenic impacts on the terrain had a greater effect on the thermal regime of permafrost than climate change (Pavlov and Moskalenko 2001). Surface disturbances are accompanied by a considerable increase in the depth of seasonal thawing and surface subsidence. Waterlogged sites in permafrost areas show varying diurnal methane fluxes, which is related to the specific thermal regime (Nakano *et al.* 2000).

A high number of lakes also exist in lowlands of the boreal severe climate of the middle east of the Siberia II area where ground ice contents are comparably high, similar to the Taymir lowlands (Stolbovoi and McCallum 2002). These features do not occur in the remaining parts, but several large water reservoirs are located in the boreal continental zone. Salt lakes occur in the steppe of the south west. The Yenisei river basin makes up 60 % of the Siberia II region. Other watersheds are tributaries to the Kolyma and Lena River and there are some smaller catchments on the Taymir peninsula.

Figure 1

Methodology

Validation data

Information on water surfaces is included in a forest inventory database provided by Russian forest enterprises. They are based on ground surveys and aerial photo interpretations, and are available as GIS layers. This database constitutes the most accurate and detailed ground data currently available. However, the inventoried sites only form a small proportion of the area covered in this study (1.5 %), and are mostly confined to features finer than the resolution (150 m) of the used satellite images.

Therefore additional data has been used for validation, specifically these are 1) a MODIS land cover map; 2) a water body map derived from topographic maps; 3) a digital chart of the world and 4) a global lakes and wetlands database. All validation data are summarized in Table 1. The MODIS land cover map derived within Siberia II project (Schmullius *et al.* 2003) is used for comparison. The water bodies map is based on topographic maps and was provided by IIASA (International Institute of Applied System Analysis). These maps date back to the 1970s, and therefore do not show recent changes due to human impact and natural dynamics. The digital chart of the world (DCW) is a global vector dataset, which is provided by the Environmental Systems Research Institute, Inc. (ESRI). The Global Lakes and Wetlands Database (GLWD) by Lehnert and Döll (2004, distributed by the World Wildlife Fund), is a recent compilation of a range of datasets, including the DCW. Within the Siberia II area, the water classes (lakes, reservoirs and rivers) are mostly based on the DCW. However, recent information on the extent of new reservoirs has been included in form of circular features, which represent the same surface area as reported in national digital databases (based on topographic maps, see Fig. 2). This allows the accounting of water on a general level such as ecoregion summaries. Additionally, georeferenced Landsat7-ETM+ data, provided by the Global Land Cover Facility of the University of Maryland, are used for a visual, qualitative assessment. A further dataset with water bodies of sufficient resolution is the Version 2 SRTM Water Body Dataset (SWBD, 90m). It is, however, limited to regions south of 60N.

Table 1: Available digital validation data which contain a water class distributed by the WWF or available to the project through IIASA and University of Wales.

Sensor and satellite data

ENVISAT was launched by ESA (European Space Agency) in February 2002, into a sun synchronous orbit, at about 800 km altitude and an inclination of 98.55°. The ASAR (Advanced Synthetic Aperture Radar) instrument is one of the instruments installed aboard. It provides radar data in different modes with varying spatial resolution and alternating polarisations in C-Band (~5.6 cm wavelength). This study utilises ASAR data acquired in Wide Swath (WS) mode at VV polarisation. The acquired images have a pixel spacing of 75 m which corresponds to an approximate spatial resolution of 150 m. Each swath covers an area of 405 km width. All available images were acquired on ascending orbits. More than 500 scenes are available for central Siberia for the years 2003 and 2004, most of them are acquired during the winter period. Therefore only about 100 scenes each, were processed for the summer periods (July and August) 2003 and 2004. Together, they provide an almost complete coverage (95%), enabling mapping of open water surfaces for the whole study area.

Pre-processing

The ASAR WS images are swath partitions of approximately 405 km in length (Desnos *et al.* 2000). For further processing these data have to be georeferenced with respect to earth curvature and the topography (Meier *et al.* 1993). Digital elevation data of sufficient resolution are only available below 60°N from the Shuttle Radar Topography Mission (SRTM, 100 m x 100 m). However, since wetlands occupy mostly flat regions, and the topography in the study area is moderate in higher latitudes, the earth curvature based correction is sufficient. Additionally, the effects due to varying incidence angel and distance from sensor (near and far range) have been removed from the backscatter measurements (Roth *et al.* 1993, van Zyl *et al.* 1993).

Classification of open water surface areas

Open water surfaces larger than 2 ha can readily be identified using a simple threshold based classification applied to the normalized image data (Figure 3). Specular reflection (away from sensor) from calm water surfaces results in low backscatter. This phenomenon enables a straight forward identification of inundation in areas with limited vegetation coverage. Inundation patterns in turn, are the key to wetland detection when using radar data.

Thresholds are set to separate areas of low, medium and high backscatter. The threshold values are chosen independently from acquisition date or location. It should be noted that this approach limits the detection of large water bodies at some dates due to wind action, but enables efficient processing of the large amount of data. Low values, similar to specular reflection from water, can occur in regions of radar shadow. As this effect only occurs in terrain where lakes are not expected, these regions are excluded from further analysis. The regions affected are derived from SRTM and GTOPO30 digital elevation data and cover 20% of the Siberia II area.

Post-processing for wetland detection and methane accounting

Permanent open water bodies play an important role in wetland identification where they are shallow. This is often related to abundance. This means not simply abundance of water, but a high density of single (small) features. Permanently inundated basins, below a size of 8 ha, in the sub-arctic regions, indicate tundra wetlands according to the Ramsar classification scheme (Frazier 1999). To perform a density analyses, these features were separated from the complete classification result. Based on information from topographic maps a density threshold has been set to 5,000 m^2 km^{-2} of water surface area from ASAR WS derived features between 2 and 8 ha for the delineation of Ramsar wetland type Vt. It is referred to as 'Method 1' below. Since no full ASAR WS coverage was available to provide this information with respect to the Ramsar classification scheme (lakes < 8 ha) for the entire sub-arctic zone of the study area, an alternative approach has been developed. This approach (Method 2) makes use of the differing spatial scale of the MODIS land cover and the ASAR WS water bodies map. In a first step, all lakes are selected with a size below approximately 30 ha from the ASAR WS water bodies layer. Then all lakes which overlap with the tundra area as classified with MODIS (500m pixel spacing) have been extracted. The same density analysis as described above for the tundra ponds (Method 1) was carried out for the selected features.

One major requirement for use in GHG accounting based on the GIS approach as pursued by IIASA is complete coverage over the study region. Since ASAR WS data are only available for 95% of the region, gaps need to be filled with other data. Most appropriate are the Russian base data, although they are generalized and only contain features larger than 10 ha.

Therefore, the ASAR WS water layer was post-processed in order to provide spatial continuity over the entire area. Morphology operations were used for eliminating noise components in the binary image (erode followed by dilate using a 3 x 3 window). The resulting image contained features larger than approximately 5 ha and was then converted to vector format (polygons), which allowed the selection of features with a minimum size of 10 ha, as available from the Russian base data. Gaps were identified and the corresponding information was selected from the Russian base data. Finally both layers were merged.

Grid based ecosystem models require input on coarser resolution (e.g. 0.5° by LPJ-DGVM, e.g. Beer *et al.* 2006). Other land cover products by Siberia II contain information on 500 m pixel spacing. Therefore a layer of fraction of inundation has been produced on this level of detail (500m x 500m).

Results

Table 2 lists the percentage and proportion of lakes found in each landscape group resembling different climatic zones. The statistics are based on the combined layer with features > 10 ha. The northern region, with an arctic and sub-arctic tundra environment, has a high percentage of water coverage, and more than 39,000 water bodies, as identified by ASAR WS. If smaller detectable lakes (2-8 ha) are taken into account the number of lakes in the sub-arctic moderate zone rises to more than 150,000, which totals to 2,500 km² of additional water surface for natural lakes.

Table 2: Distribution of water bodies > 10 ha by landscape group for a) all water bodies and b) natural inundated basins only, this excludes large rivers and reservoirs

Figure 2

Figure 3

Regions where surface water from small lakes (2 - 8 ha) adds up to more than 5000 m^2 km^{-2} are shown in

Figure 4. The tundra wetlands, as defined by the second method (use of ASAR WS water bodies within MODIS tundra class), cover approximately 400,000 km^2 which corresponds to more than 7% of the entire Siberia II study region. All Ramsar Wetlands of International Importance on south-western Taymir are located within the ASAR WS derived tundra wetland zone (Bartsch *et al.* 2007). The mean density for the Pura/Gorbitta site is approximately 5800 m^2 km^{-2} by lakes between 2 and 8 ha size. The mean density for larger lakes up to 30 ha, derived by the Method 2 (10-30ha within MODIS tundra class) within Pura/Gorbitta is ca. 7000 m^2 km^{-2} (Table 3). This information can serve as input for waterfowl habit identification (Bartsch *et al.* 2007).

Table 3: Interpolated water density (radius 10 km) in m^2 km^{-2} for the Pura/Gorbitta Wetland Area of International Importance

Qualitative assessment

Topographic maps were used for visual evaluation of the classification result. There are some discrepancies since these maps date back to the 1970s and therefore do not show recent changes due to human impact and natural dynamics. The ASAR WS water bodies map provides an update on these changes. One example is shown in

Figure 2. The area of the reservoir created at the Kureika River mapped by the GLWD (Lehner and Döll 2004), only shows up as a circular feature since its exact boundaries were not known but only its size of 511 km². In comparison, ASAR WS identifies 517 km² for the reservoir surface in summer 2003.

Quantitative assessment and cross comparison

80 % of all water areas mapped in the inventory could be identified with ASAR WS compared to the Russian forest inventory data. Features not identified are rivers, which are below ASAR WS resolution, and water bodies which lack sufficiently smooth surface conditions during the acquisition of the ASAR WS images. A detailed assessment has been carried out for the Norilsk test site, where a sufficient number of lakes and rivers can be found (Santoro et al. 2004). The test site has a size of ca. 640 km². The extent of water surfaces as classified from ASAR WS is approximately 100 km² (Fig. 5). The result is assessed using the Kappa coefficient (e.g. Congalten and Green 1999) as a measure of reliability of the classification accuracy. The Kappa coefficient is 0.82 with an overall classification accuracy of 95%.

Figure 4

Figure 5

The opposite effect (as found with the detailed forest inventory data) occurs when comparing the results with the MODIS derived land cover data since their spatial resolution is coarser. Only 50% (in relation to ASAR WS) of water surface area is identified at the MODIS 500 m resolution. This agrees with assessments within the northern parts of the adjacent West Siberian Lowlands (Frey and Smith 2007).

Figure 6 shows the result of a comparison with MODIS level 2 land cover classes. The area in km² of open water derived from ASAR WS within each MODIS land cover class is shown. Less than 1000 km² coincide with the MODIS water class. It can be clearly seen that most confusion occurs in the Tundra area (9500 km² of open water surfaces), where small features below the MODIS resolution are dominant (Bartsch *et al.* 2004). The largest absolute differences occur within ecoregion 'k601' which is located in the sub-arctic and arctic biome (see Fig. 1). Within this region and the adjacent k401 and k1602 less then 10 % of ASAR water bodies are detected by MODIS. More detail and additional information is gained in comparison to the GLWD (see

Figure 2 and Figure 7). Tundra wetlands itself are not considered by the MODIS classification scheme.

Figure 6

Figure 7

Methane emissions from tundra and boreal lakes in regions of high ice content in permafrost

A mean methane emission from tundra lakes of 3.5 mg m^{-2} day^{-1} has been measured near Tarko-Sale, Western Siberia, (Gal'chenko *et al*. 2001) and 7.6 mg m^{-2} day^{-1} in the Kolyma Lowlands, Yakutia, North-eastern Siberia (Zimov *et al.* 1997). Applying these numbers to the results of the ASAR WS classification, this would add up to an emission of ca. 9 t day^{-1} and 19 t day^{-1} respectively, for permanent lakes within the moderate subarctic zone of the

Siberia II area. According to Zelenev (1996) approximately 120 mg m^{-2} day^{-1} of methane are emitted on average from hydromorphic tundra soils (Gleysols in permafrost) found in this region (Stolbovoi and McCallum 2002). This adds up to about 45,000 t day^{-1} of methane emission from the Taymir wetlands during the growing season. Although the contribution of methane from lakes is much lower than that of the surrounding wetland area in summer, emissions from lakes continue during winter and the quantification of their spatial extent is therefore of importance. If seen in relation to the estimate by Zhuang *et al.* (2004) of 51 Tg yr^{-1} for the arctic environments, the Taymir contribution equals approximately a quarter of total high latitude methane emissions and 40% of Russia's arctic net methane emissions respectively. The extent of tundra wetlands in general, however, is underestimated in the database used by Zhuang *et al*. (2004), therefore the overall emissions might be higher and thus the contribution from the Taymir lowlands lower.

Discussion

ASAR WS data provide detailed and precise information on permanent inundation over large areas. For applicability on global scale, however, data availability is crucial. The observation frequency would theoretically allow the investigation of dynamics related to hydrological changes on a global scale. Practically the application of the technique is however limited to regional scale analysis by the competing acquisition modes of the ASAR instrument. Only one of the modes, Image, Alternate Polarisation, Wide Swath or Global Mode can be requested at one time from ENVISAT. Using Global Mode data might be a solution for this problem. The repetition rate of Global Mode is comparably high over central Siberia as it is operated permanently as background mode whenever there is no specific acquisition requested (Bartsch *et al.* in press). The spatial resolution of 1 km also allows operational processing on global scale at reasonable cost (Wagner *et al.* 2007). However, the coarse resolution may constrain the applicability of the data for hydrological purposes on the level of detail required for tundra wetlands monitoring as presented in this paper.

Inter-annual variability could not be assessed since there is insufficient spatial overlap between data from 2003 and 2004 in the thermokarst affected regions. Changes might occur due to thermokarst dynamics and permafrost degradation as identified with Landsat-TM data by Frohn *et al.* (2005) and by Stow *et al.* (2004) respectively for Alaska.

Land cover data which are used for ecosystem models are based on comparably coarse resolution satellite data such as from MODIS or MERIS data (GLCC, GLOBCOVER etc.). In order to enhance their level of detail, the ASAR WS classification results can be provided on the same pixel spacing using water fraction instead of binary information (water or non-water, see Fig. 8). This can then be used for global dynamic vegetation models such as LPJ-DGVM (Beer *et al.* 2006). Although data in wide swath mode are sufficient to map small tundra ponds, polygon mire systems cannot be captured directly. This requires finer resolution as low as 2.5 m (Grosse *et al.* 2005, data source CORONA) what is beneficial for local studies but not feasible on regional or global scale. Additional to the density of lakes and water fraction, information for carbon accounting can be derived from lake size itself (Kortelainen *et al.*

2004) as demonstrated for a SAR (JERS-1) based analyses over Canada by Thelmer and Costa (2007).

Figure 8

Compared to methane emissions from wet tundra soil the daily contribution from shallow lakes seems to play a minor role, but methane is also emitted during winter time from these small tundra lakes. Zimov *et al.* (1997) estimated that 75% of fluxes from Siberian lakes occur during winter time what roughly corresponds to its length throughout the tundra biome. This underlines the importance to quantify the winter fluxes. The required ground measurements, however, are scarce. Climate change impacts especially the length of the growing season. With that, the weight of shallow lakes and moist tundra soils with respect to greenhouse gas accounting is shifted. Apart from such seasonal changes, the spatial distribution of these water bodies underlies variation. Thermokarst formation may be intensified by increasing length of the growing season (Ostercamp and Romanovsky 1999), which supports the formation of lakes in the first moment when water becomes available from thawing permafrost where topography permits this development (Callaghan *et al.* 2004). This supports carbon sequestration under anaerobic conditions. If this water supply ceases and water tables are lowered, however, this process might be reversed and CO_2 will be released whilst CH_4 emissions will be reduced (Gorham 1991). Diverse patterns of peat accumulation in relationship to local topography and ground ice contents make predictions of climate change difficult. A high level of detail concerning hydrological dynamics could be provided by ASAR WS on global scale which may enhance such assessments.

Conclusions

Although there are only limited data for a quantitative assessment available, it can be concluded that the ASAR WS water bodies map provides sufficiently accurate (Kappa > 0.8) and especially up to date information. Additional information is gained for sub-arctic environments when compared to MODIS derived land cover. Regions which have been so far classified as tundra (or included in 'grasslands and shrubs' on MODIS level 1) are characterized by numerous small shallow inundated basins, which coincide with a specific wetland type in this environment.

The chosen approach has been proven applicable over a large area and can be expanded in order to derive information for the entire circum polar region. Data fusion allows the integration of these data into GHG accounting data bases in form of measure of 1) water fraction as considered in dynamic global vegetation models (such as LPJ or SDGVM) or 2) vector based as required by the IIASA GIS landscape ecosystem approach (Bartsch *et al.* 2004).

The extent of freshwater ecosystems in the Tundra zone can be derived from either solely ENVISAT ASAR WS or in combination with MODIS land cover maps. Tundra wetlands account for 7% of the central Siberian region. The derived layers (wetlands and water bodies) form a valuable base for monitoring these habitats and determination of carbon cycle components.

Acknowledgements

This research has been carried out in connection with two research projects: MISAR and Siberia II. The latter is a shared-cost action financed through the 5th Framework Program of the European Commission, Generic Activity 7.2: Development of generic Earth Observation Technologies (EVG1-CT-2001-00048). The MISAR project was financed by the Austrian Science Fund (P16515-N10). ASAR WSM data are available by courtesy of ESA and SRTM3 by USGS.

References

Andreev, A. A., Siegert, C., Klimanov, V. A., Derevyagin, A. Y., Shilova, G. N. and Melles, M. (2002). Late Pleistocene and Holocene Vegetation and Climate on the Taymir Lowland, Northern Siberia. *Quaternary Research,* **57**, 138-150.

Bartsch, A., Kidd, R., Pathe, C., Shvidenko, A. and Wagner, W. (2004). Identification of wetlands in central Siberia with ENVISAT ASAR WS data. *Proceedings ENVISAT Symposium*, Salzburg, Austria, 6-10 September 2004, ESA SP-572.

Bartsch, A., Kidd, R., Pathe, C., Scipal, K. and Wagner, W. (2007). Satellite radar imagery for monitoring inland wetlands in boreal and sub-arctic environments. *Aquatic Conservation: Marine and Freshwater Ecosystems, **17**, 305-317*.

Bartsch, A., Wagner, W., Scipal, K., Pathe, C., Sabel, D. and Wolski, P. (in press). Global monitoring of wetlands – the value of ENVISAT ASAR global mode. *Journal of Environmental Management.*

Beer, C., Lucht, W., Schmullius, C. and Shvidenko, A. (2006). Small net carbon dioxide uptake by Russian forests during 1981-1999. *Geophysical Research Letters,* **33**, L15403.

Callaghan, T. V., Björn, L. O., Chernov, Y., Chapin, T., Christensen, T. R., Huntley, B., Ims, R. A., Johansson, M., Jolly, D., Jonasson, S., Matveyeva, N., Panikov, N., Oechel, W., Shaver, G., Schaphoff, S. and Sitch, S. (2004). Effects of Changes in Climate on Landscape and Regional Processes, and Feedbacks to the Climate System. *Ambio,* **33** (7), 459-468.

Congalton, R. G. and K. Green (1999). *Assessing the Accuracy of Remotely Sensed Data: Principles and Practices*. Lewis Publishers, Boca Raton.

Desnos, Y.-L., Buck, C., Guijarro, J., Suchail, J.-L., Torres, R. and Attema, E. (2000). ASAR- Envisat´s Advanced Synthetic Aperture Radar. Building on ERS Achievements towards Future Watch Missions. *ESA Bulletin,* **102**, 91-100.

Christensen, T. R., Johansson, T., Åkerman, H. J., Mastepanov, M., Malmer, N., Friborg, T., Crill, P. and Svensson, B. H. (2003). Thawing sub-arctic permafrost: Effects on vegetation and methane emissions. *Geophysical Research Letters,* **31**, L04501.

Frazier, S. (Ed.)(1999). *Ramsar Sites Overview - A Synopsis of the World's Wetlands of International Importance*. Wetlands International.

Frey, K. E. and L. C. Smith (2007). How well do we know northern land cover? Comparison of four global vegetation and wetland products with a new ground-truth database for West Siberia. *Global Biogeochemical Cycles*, **21**, GB1016.

Friborg, T., Soegaard, H., Christensen, T. R., Lloyd, C. R. and Panikov, N. S. (2003). Siberian wetlands: Where a sink is a source. G*eophysical Research Letters,* **30** (21), 2129.

Frohn, R. C., Hinkel, K. M. and Eisner, W. R. (2005). Satellite Remote Sensing Classification of Thaw Lakes and Drained Thaw Lake Basins on the North Slope of Alaska. *Remote Sensing of Environment,* **97**, 116-126.

Gal'chenko, F. V., Dulov, L. E., Cramer, B., Konova, N. I. and Barysheva, S. V. (2001). Biogeochemical Processes of Methane Cycle in the Soils, Bogs, and Lakes of Western Siberia. *Microbiology,* **70** (2), 215-225.

Gorham, E. (1991). Northern Peatlands: Role in the Carbon Cycle and Probable Responses to Climate Warming. *Ecological Applications,* **1**(2), 182-195.

Grosse, G., Schirrmeister, L., Kunitsky, V. V. and Hubberten, H.-W. (2005). The Use of CORONA Images in Remote Sensing of Periglacial

Geomorphology: An Illustration from the NE Siberian Coast. *Permafrost and Periglacial Processes,* **16**, 163-172.

Kortelainen, P., Pajunen, H., Rantakari, M. and Saarnisto, M. (2004). A large carbon pool and small sink in boreal Holocene lake sediments. *Global Change Biology,* **10**, 1648-1653.

Krinner, G. (2003). Impact of Lakes and Wetlands on Boreal Climate. *Journal of Geophysical Research,* **108** (D16), 4520.

Laing, T. E. and Smol, J. P. (2003). Late Holocene Environmental Changes Inferred from Diatoms in an Lake on the Western Taimyr Peninsula, Northern Russia. *Journal of Paleolimnology,* **30**, 231-247.

Lehner, B and Döll, P. (2004). Development and Validation of a Global Database of Lakes, Reservoirs and Wetlands. *Journal of Hydrology,* **296,** 1 – 22.

McCallum, I., Obersteiner, M., Nilsson, S. and Shvidenko, A. (2006). A spatial comparison of four satellite derived 1 km global land cover datasets. *International Journal of Applied Earth Observation and Geoinformation,* **8**(4), 246-255.

Meier, E., Frei, U. and Nüesch, D. (1993). Precise Terrain Corrected Geocoded Images. In: Schreier, G. (ed.) *SAR geocoding: data and systems*. Wichmann, Karlsruhe.

Mitra, S., Wassmann, R. and Vlek, P. L. G. (2005). An Appraisal of Global Wetland Area and its Organic Carbon Stock. *Current Science,* **88**(1), 25-35.

Nakano, T., Kuniyoshi, S. and Fukuda, M. (2000). Temporal Variation in Methane Emissions from Tundra Wetlands in a Permafrost Area, Northeastern Siberia. *Atmospheric Environment,* **34**, 1205-1213.

Osterkamp, T. E. and Romanovsky, V. E. (1999). Evidence for Warming and Thawing of Discontinuous Permafrost in Alaska. *Permafrost and Periglacial Processes,* **10**, 17-37.

Pavlov, A. V. and Moskalenko, N. G. (2002). The Thermal Regime of Soils in the North of Western Siberia. *Permafrost and Periglacial Processes,* **13**, 43-51.

Roth, A., Craubner, A. and Hügel, T. (1993). Standard Geocoded Ellipsoid Corrected Images. In: Schreier, G. (ed.) *SAR geocoding: data and systems*. Wichmann, Karlsruhe.

Santoro, M., Schmullius, C., Balzter, H., Bartsch, A., Grippa, M., Kidd, R., Le Toan, T., L'Hermitte, J., Petrocchi, A., Roscher, M., Rowland, C., Voigt, S., Wagner, W., Wegmüller, U. and Wiesmann, A. (2004). The Siberia-II project as seen by ENVISAT ASAR. *Proceedings of the CEOS SAR '04 Workshop*, Ulm 27-28 May.

Schmidt, N. and Bölter, M. (2002). Fungal and Bacterial Biomass in Tundra Soils Along an Arctic Transect from Taimyr Peninsula, Central Siberia. *Polar Biology,* **25**, 871-877.

Schmullius, C., Hese, S. and Knorr, D. (2003). Siberia-II - A Multi Sensor Approach for Greenhouse Gas Accounting in Northern Eurasia. *Petermanns Geographische Mitteilungen,* **147** (6), 4-5.

Stolbovoi, V. and McCallum, I. (2002). CD-ROM "*Land Resources of Russia*", International Institute for Applied Systems Analysis and the Russian Academy of Science, Laxenburg, Austria.

Stolbovoi, V. S., Nilsson, S., Shvidenko, A. Z. and McCallum, I. (2004). Aggregated Estimation of Basic Parameters of Biological Production and Carbon Budget of Russian Terrestrial Ecosystems: 3. Biogeochemical Carbon Fluxes. *Russian Journal of Ecology,* **35** (3), 150-155.

Stow, D. A., Hope, A., McGuire, D., Verbyla, D., Gamon, J., Huemmerich, F., Houston, S., Racine, C., Sturm, M., Tape, K., Hinzman, L., Yoshikawa, K., Tweedie, C., Noyle, B., Silapaswan, C., Douglas, D., Griffith, B., Jia, G., Epstein, H., Walker, D., Daeschner, S., Petersen, A., Zhou, L. and Myneni, R. (2004). Remote Sensing of Vegetation and Land-Cover Change in Arctic Tundra Ecosystems. *Remote Sensing of Environment,* **89**, 281-308.

Telmer, K. H. and Costa, M. P. F. (2007). SAR-based estimates of the size distribution of lakes in Brazil and Canada: a tool for investigating carbon in lakes. *Aquatic Conservation: Marine and Freshwater Ecosystems,* **17**, 289-304.

Tumel, N. (2002). Permafrost. In: Shahgedanova, M. (ed.) *The Physical Geography of Northern Eurasia*. Oxford University Press, Oxford.

Wagner, W., Pathe, C., Sabel, D., Bartsch, A., Künzer, C. and K. Scipal (2007). Experimental 1 km soil moisture products from ENVISAT ASAR for Southern Africa. *Proceedings of the ENVISAT Symposium*, Montreux 2007.

Zelenev, V. V. (1996). Assessment of the Average Annual Methane Flux from the Soils of Russia. WP-96-51, International Institute for Applied Systems Analysis, Laxenburg.

Zhuang, Q., Melillo, J. M., Kicklighter, D. W., Prinn, R. G., McGuire, A. D., Steudler, P. A., Felzer, B. S. and Hu, S. (2004). Methane Fluxes between Terrestrial Ecosystems and Atmosphere at Northern High Latitudes During the Past Century: A Retrospective Analysis with a Process-Based Biogeochemistry Model. *Global Biogeochemical Cycles,* **18**, GB3010.

Zimov, S. A., Voropaev, Y. V., Semiletov, I. P., Davidov, S. P., Prosiannikov, S. F., Chapin III, F. S., Chapin, M. C., Trumbore, S. and Tyler, S. (1997). North Siberian Lakes: A Methane Source Fuelled by Pleistocene Carbon. *Science,* **277**, 800-802.

van Zyl, J., Chapman, B., Dubois, P. and Shi, J. (1993). The effect of the topography on SAR calibration. *IEEE Trans. Geoscience Rem. Sens*., **31**(5), 1036-1043.

Database	availability	source	resolution/scale
Forest inventory	selected sites	Aerial photographs, field surveys, IIASA	< 1 : 10 000
vector water layer	national	topographic maps, IIASA	1 : 200 000 features > 10 ha
MODIS landcover	Siberia II area	MODIS classification, UWS	500 m
GLWD	global	diverse, Lehner and Döll 2004	features > 10 ha

Table 1: Available digital validation data which contain a water class distributed by the WWF or available to the project through IIASA, Laxenburg and University of Wales, Swansea (UWS)

Landscape group (climatic zone)	**a) all water bodies in % of Siberia II area**	**b) natural lakes**		
		in % of Siberia II area	**sum area km²**	**number**
arctic	3.95	2.33	5254	3921
sub-arctic moderate	8.44	5.16	20383	35900
sub-arctic severe	1.05	0.44	1989	2376
boreal continental	1.37	0.16	2469	4383
boreal severe	0.37	0.22	1010	1901
sub-boreal (steppe)	4.30	0.71	413	437
Sum for Siberia II area	19.00	9.00	31518	48918

Table 2: Land coverage of water bodies > 10 ha for each landscape group for a) all water bodies and b) natural inundated basins only, excluding large rivers and reservoirs

source for density analysis	**mean**	**min**	**max**	**standard deviation**
2 – 8 ha tundra ponds	5786	269	41003	4947
< 30 ha & MODIS tundra	7121	1830	15270	2077

Table 3: Interpolated water density (within a circle with radius of 10 km) in $m^2\ km^{-2}$ for the Pura/Gorbitta Wetland Area of International Importance

Figure 1: Natural lakes, reservoirs and rivers of the Siberia II region– final result; with GHG accounting ecoregions and climate zones

Figure 2: The new Kureika River reservoir. Comparison of ASAR WS water bodies with global (GLWD, Lehner and Döll 2004) and national (based on topographic maps) digital databases.

Figure 3: Threshold classification example a Tundra site: a) greyscale normalized image, b) classified image with lakes in grey and c) histogram of normalized backscatter in dB

Figure 4: Tundra wetland zone derived from ASAR open water features; method 1: in combination Russian base data density analyses of lakes 10 – 30 ha which are classified as tundra in the MODIS land cover layer, method 2: density analysis of lakes 2 – 8 ha where ASAR WS is available in accordance with the Ramsar wetland classification scheme

Figure 5: Norilsk validation site: a) Forest Inventory units and water class plus water bodies from a 1:1 Mio map (both provided by IIASA); b) Comparison of water bodies between ASAR WS and MODIS land cover (from UWS).

Figure 6: Area (in km^2) of water bodies per MODIS level 2 land cover class for final water layer (natural lakes only)

Figure 7: Comparison of water surface area in ASAR WS (final product, incl. added information from topographic maps) and the GLWD 2004 by ecoregion (for location see Figure 1)

Figure 8: Permanent water bodies of the Taymir lowlands, a) Water fraction map derived from ASAR WS water bodies classification, b) Rivers and lakes as available from the Global lakes and wetlands database (Lehner and Döll 2004)

Figure 1

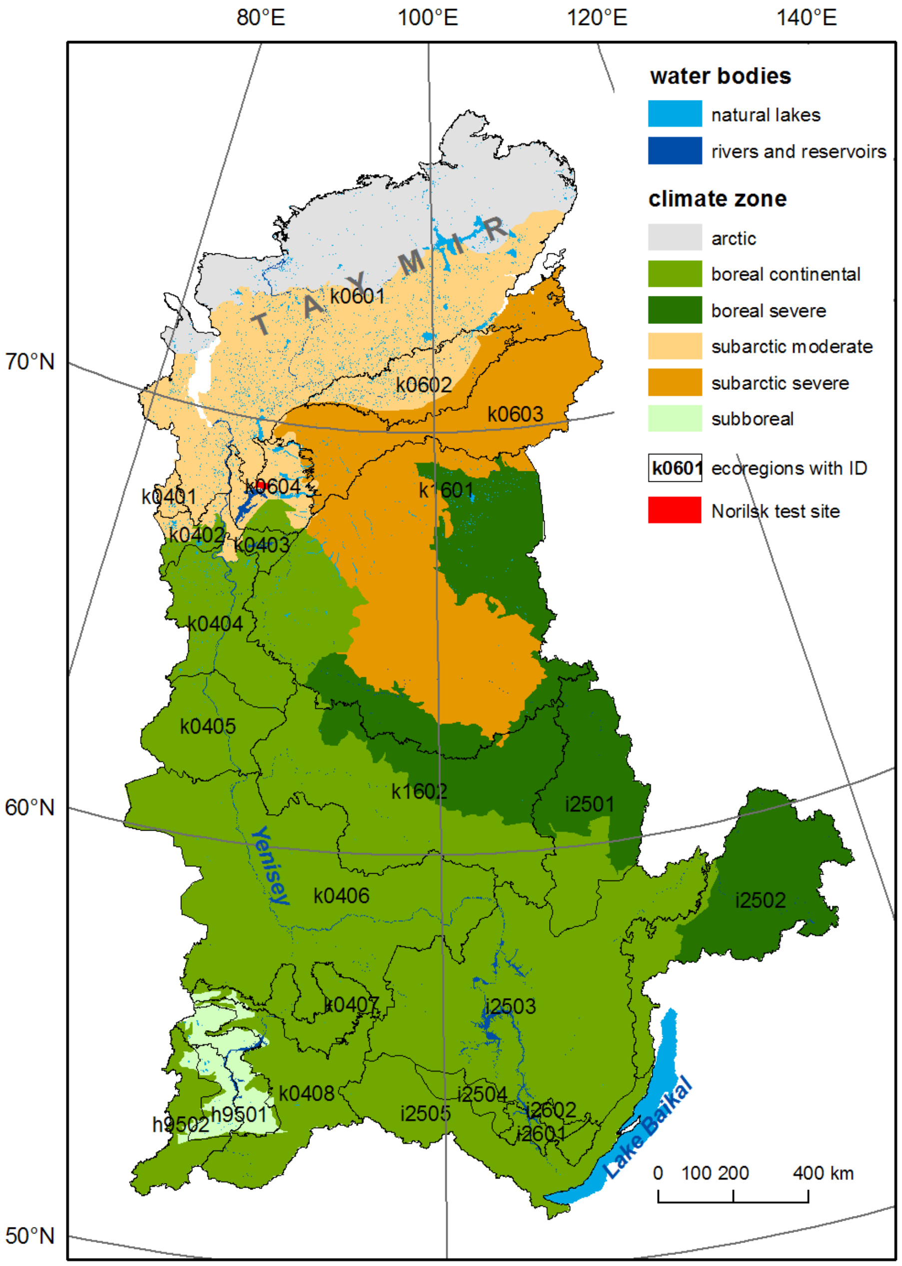
80°E
100°E
120°E
140°E
70°N
60°N
50°N
water bodies
natural lakes
rivers and reservoirs
climate zone
arctic
boreal continental
boreal severe
subarctic moderate
subarctic severe
subboreal
k0601 ecoregions with ID
Norilsk test site
T A Y M I R
k0601
k0602
k0603
k0604
k0401
k0402
k0403
k1601
k0404
k0405
k1602
i2501
Yenisey
k0406
i2502
k0407
i2503
k0408
i2504
i2505
i2602
i2601
h9502
h9501
Lake Baikal
0 100 200 400 km

Figure 2

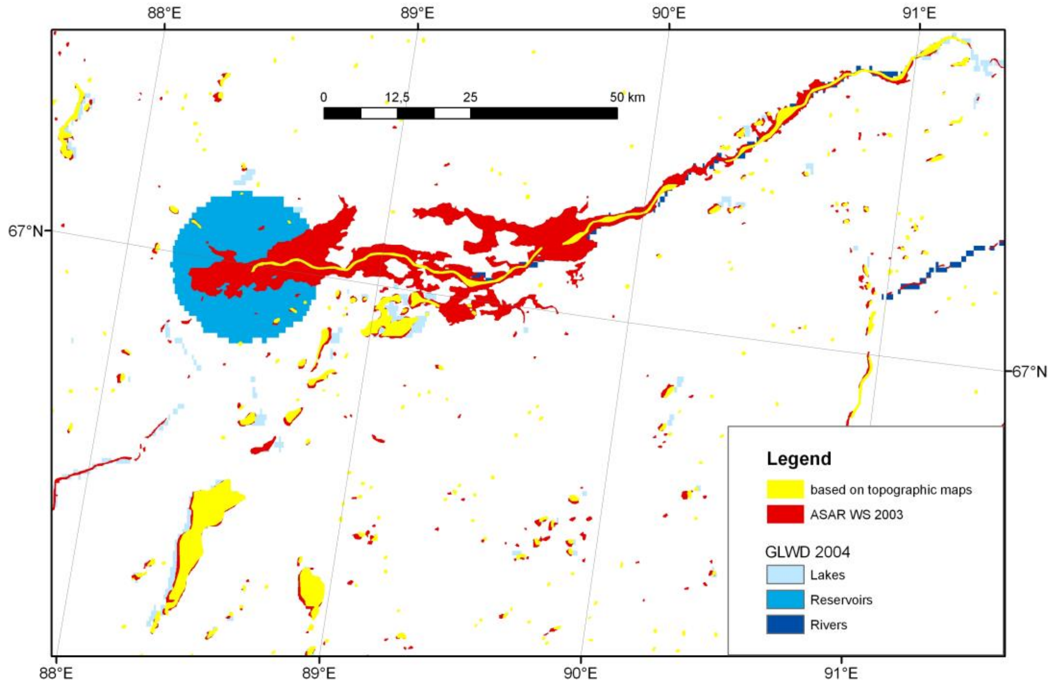
88°E
89°E
90°E
91°E
0
12,5
25
50 km
67°N
67°N
88°E
89°E
90°E
91°E
Legend
based on topographic maps
ASAR WS 2003
GLWD 2004
Lakes
Reservoirs
Rivers

Figure 3

a) 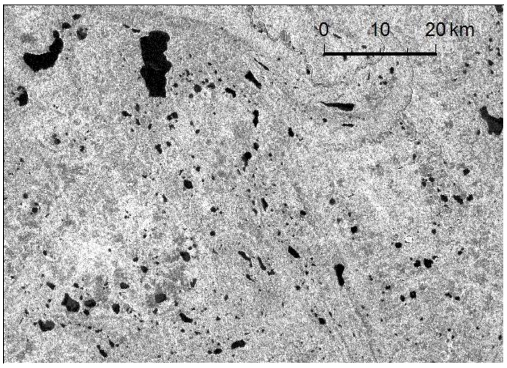
0 10 20 km

b) 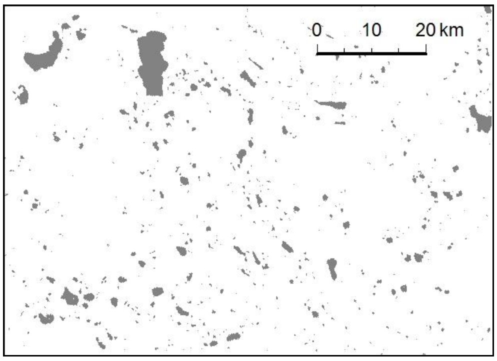
0 10 20 km

c) 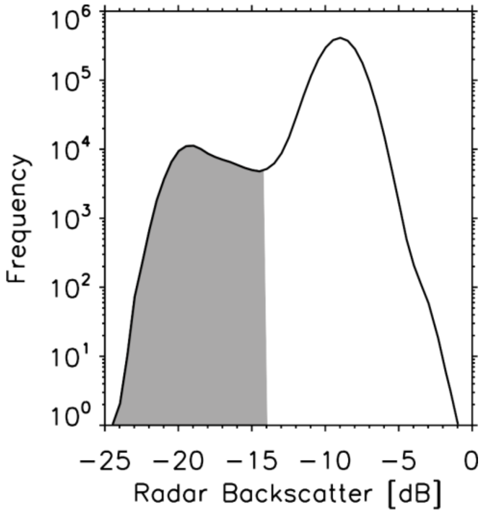
Frequency
10^6
10^5
10^4
10^3
10^2
10^1
10^0
−25 −20 −15 −10 −5 0
Radar Backscatter [dB]

Figure 4

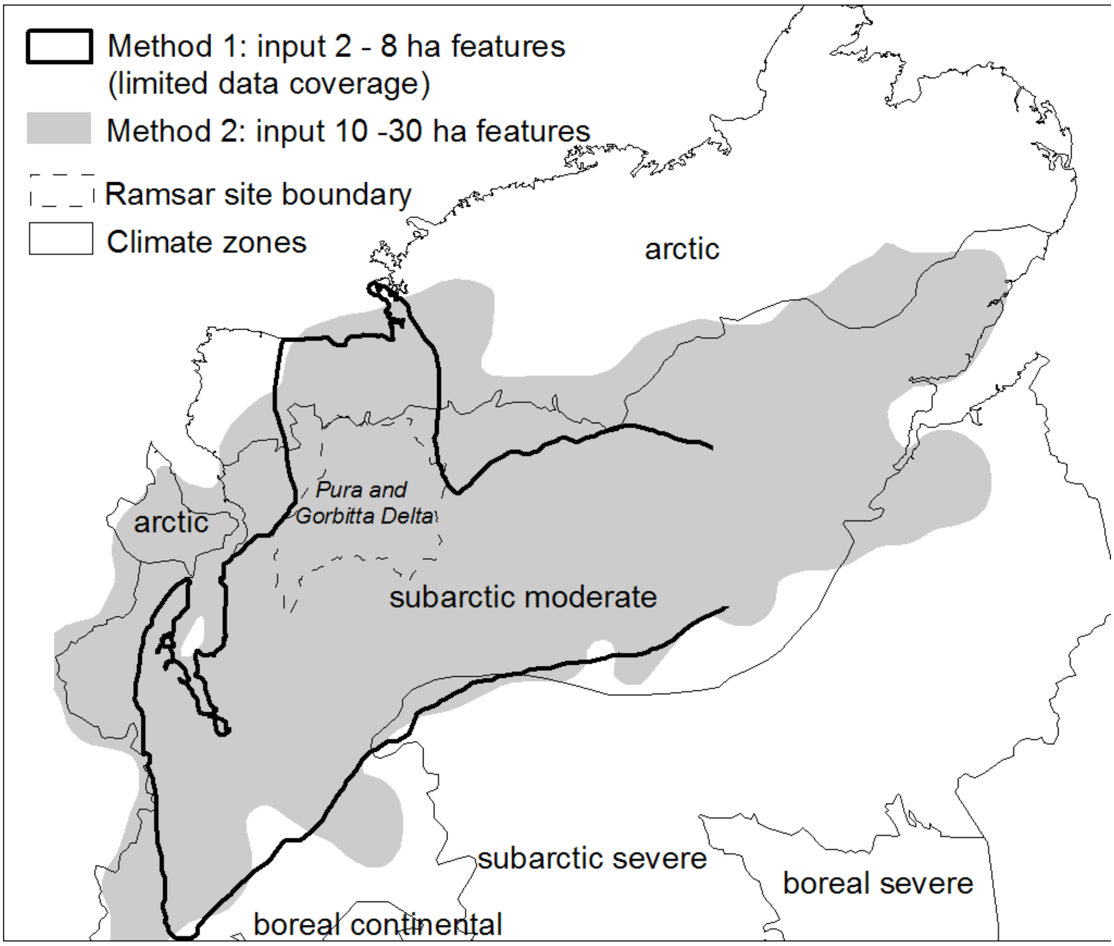
Method 1: input 2 - 8 ha features
(limited data coverage)
Method 2: input 10 -30 ha features
Ramsar site boundary
Climate zones
arctic
arctic
Pura and
Gorbitta Delta
subarctic moderate
subarctic severe
boreal severe
boreal continental

Figure 5

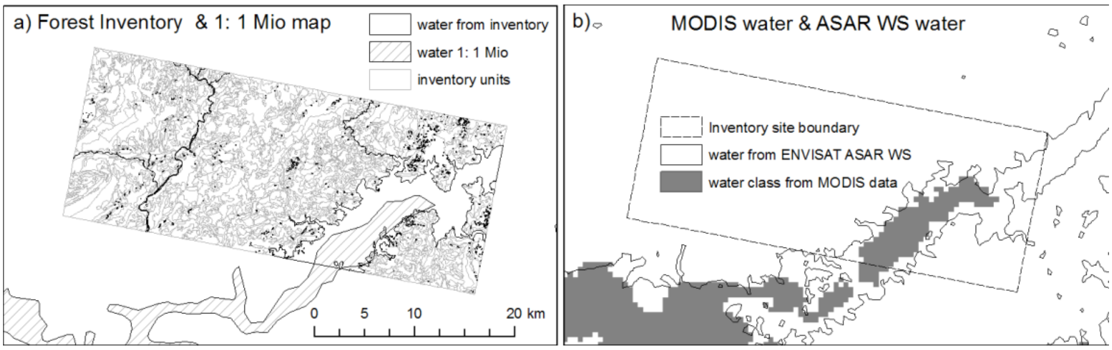
a) Forest Inventory & 1: 1 Mio map
water from inventory
water 1: 1 Mio
inventory units
0
5
10
20 km
b)
MODIS water & ASAR WS water
Inventory site boundary
water from ENVISAT ASAR WS
water class from MODIS data

Figure 6

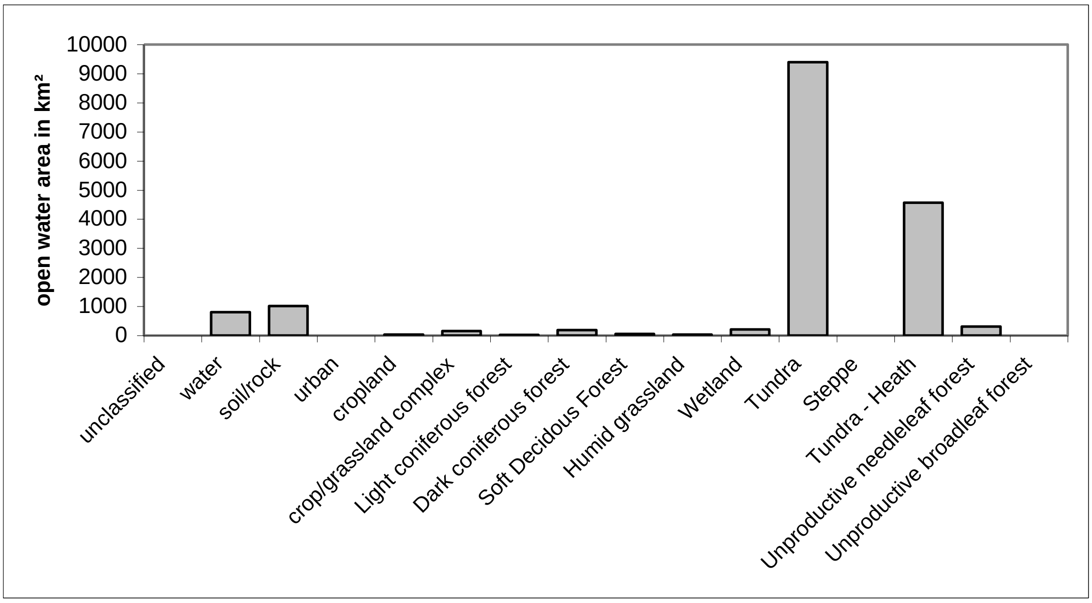
open water area in km²
10000
9000
8000
7000
6000
5000
4000
3000
2000
1000
0
unclassified
water
soil/rock
urban
cropland
crop/grassland complex
Light coniferous forest
Dark coniferous forest
Soft Decidous Forest
Humid grassland
Wetland
Tundra
Steppe
Tundra - Heath
Unproductive needleleaf forest
Unproductive broadleaf forest

Figure 7

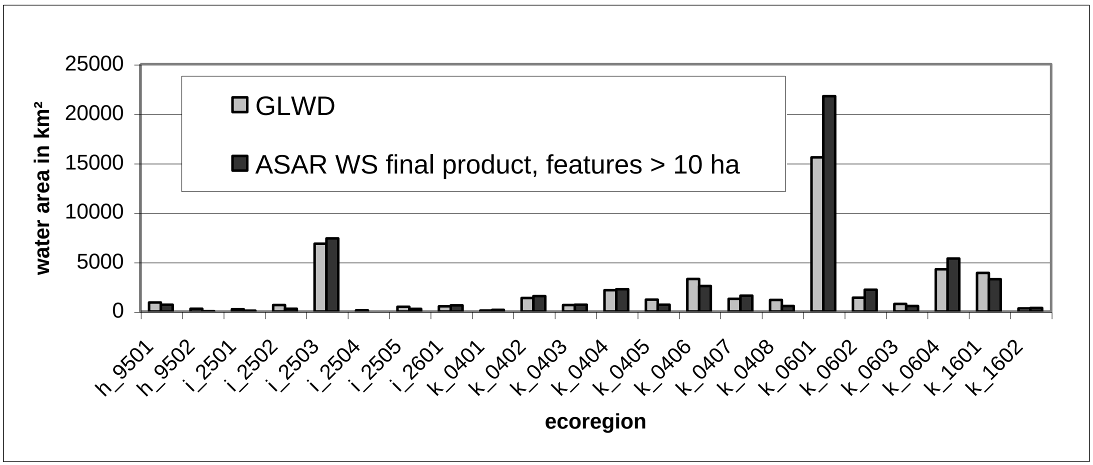
25000
20000
15000
10000
5000
0
water area in km²
GLWD
ASAR WS final product, features > 10 ha
h_9501
h_9502
i_2501
i_2502
i_2503
i_2504
i_2505
i_2601
k_0401
k_0402
k_0403
k_0404
k_0405
k_0406
k_0407
k_0408
k_0601
k_0602
k_0603
k_0604
k_1601
k_1602
ecoregion

Figure 8